

Determination of the pion-nucleon coupling constant

Gerald E. Hite

Universität Kaiserslautern, Kaiserslautern, West Germany

Richard J. Jacob and David C. Moir*

Department of Physics, Arizona State University, Tempe, Arizona 85281

(Received 19 May 1975)

A method for determining the pion-nucleon coupling constant f^2 by the application of an interior dispersion relation to the $B^{(+)}\pi N$ scattering amplitude is presented and its advantages over other dispersion relation techniques are discussed. The method is used to calculate f^2 for two sets of phase shifts: CERN 71 of Almehed and Lovelace and a modified version of the Carter, Bugg, and Carter solution, to obtain $f^2 = (81.5 \pm 1.5) \times 10^{-3}$ and $f^2 = (79.5 \pm 1.0) \times 10^{-3}$, respectively.

I. INTRODUCTION

The extraction of the pion-nucleon coupling constant, f^2 , from elastic πN scattering data has long been a basic activity of medium-energy phenomenology.¹⁻⁶ Over a period of several years, data and calculational techniques have been refined to the point where some authors have claimed precisions of the order of 1% to 2% in their estimates of the value of f^2 . Nevertheless, as seen in Table I, the variations between recently published values still exceed individual precisions, although most fall within the range of values recommended by Ebel *et al.*⁶ It is clear from a study of the various estimates of f^2 , and the procedures by which they are obtained, that an improvement in accuracy awaits more precise data and more reliable phase-shift analyses. Furthermore, the calculational techniques still contain sources of systematic errors, such as those involved in applying electromagnetic corrections and in smoothness assumptions relating to extrapolation procedures, which will restrict their credibility when applied to improved scattering information.

We present here a method for calculating the pion-nucleon coupling constant which is fundamentally different and which has distinct advantages over previous methods. Our technique, which is an application of interior dispersion relations (IDR's),⁷ is particularly well suited to the new generation of accurate low-energy scattering data now being measured at several laboratories. In the present paper, however, we perform the calculation using phase-shift analyses of current vintage, since analysis of the new data is not yet complete.

The specific advantages of the IDR method are examined in detail later in the paper. We present a summary of them here:

1. The s -channel dispersion integration is performed entirely within the physical region, elimi-

nating any need to continue amplitudes away from the region in which they were obtained by direct comparison to experimental scattering data.

2. The dispersion integral converges rapidly and may be truncated at a relatively low value of the s -channel energy. Other effects, to be described below, combine with the convergence properties to desensitize our results to d , f , and higher partial waves.

3. Variation of the path parameter a allows us to test the consistency of our results and to utilize the data over the entire range of interior angles.

4. We avoid the forward scattering region, where electromagnetic corrections are most significant.

We present our method in Sec. II, the results in Sec. III, a discussion of the merits of the technique in Sec. IV, and some relevant kinematical relationships in an appendix.

II. METHOD

In our calculation we use the amplitude

$$\tilde{B}^{(+)}(t, a) \equiv B^{(+)}(t, a)/\nu,$$

where $B^{(+)}$ is the usual isospin-even invariant am-

TABLE I. Recent determinations of f^2 from pion-nucleon data. For a review of earlier determinations, see Table 5 of Ref. 5 and Sec. 3.1 of Ref. 6.

$10^3 f^2$	Reference	Year
78.4 ± 1.0	1	1974
79.0 ± 1.0	2	1973
74.2 ± 1.3	3	1973
81.6 ± 2.9	4	1972
76.3 ± 2.0	5	1972
81_{-4}^{+3}	6 ^a	1971

^a Recommended value.

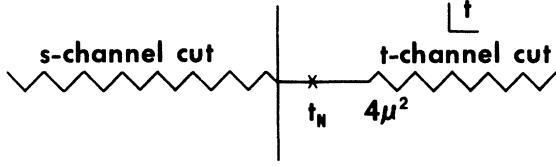


FIG. 1. The complex t plane showing the singularities which contribute to the IDR. The position of the nucleon pole, t_N , is dependent upon a .

plitude. The variables t , a , and ν are defined in the appendix. The interior dispersion relation for $\tilde{B}^{(+)}$ is written by fixing the value of a and applying Cauchy's integral formula in the complex t plane. The resulting IDR is

$$\begin{aligned} \text{Re}\tilde{B}^{(+)}(t, a) = & \tilde{B}_{\text{IDR}}^{N(+)}(t, a) + \frac{1}{\pi} \text{P} \int_{-\infty}^0 \text{Im}\tilde{B}^{(+)}(t', a) \frac{dt'}{t' - t} \\ & + \frac{1}{\pi} \text{P} \int_{4\mu^2}^{\infty} \text{Im}\tilde{B}^{(+)}(t', a) \frac{dt'}{t' - t}. \end{aligned} \quad (2.1)$$

We take $\mu = m_{\pi^+} = 0.13957$ GeV and $m = m_p = 0.9383$ GeV. The first integral in (2.1) is due to the s -channel cut ($\pi N \rightarrow \pi N$) in the t plane (see Fig. 1) and, for $a \leq 0$, corresponds to a path of integration that lies completely within the s -channel physical region. The integral converges rapidly, as we shall demonstrate in the next section, allowing us to apply the dispersion relation in an unsubtracted form. Convergence is also ensured for the second integral, which is due to the t -channel ($\pi\pi \rightarrow NN$) unitary cut. We do not attempt to calculate this integral directly from t -channel data, but simply assume that since its structure is due to singularities located at $t > 4\mu^2$ it contributes a smooth function of t at values less than this. We denote the first and second integrals by $I(t, a)$ and $D(t, a)$, respectively. A change in integration variable allows us to write

$$\begin{aligned} I(t, a) = & \frac{1}{\pi} \text{P} \int_{s_0}^{\infty} \text{Im}\tilde{B}^{(+)}(t'(s', a), a) \\ & \times \left(\frac{1}{s' - s} + \frac{1}{s' - u} - \frac{1}{s' - a} \right) ds'. \end{aligned} \quad (2.2)$$

The Born term is given by

$$\tilde{B}_{\text{IDR}}^{N(+)}(t, a) = G^2 / [(m^2 - a)(t - t_N)], \quad (2.3)$$

where

$$G^2 = 4\pi f^2 (2m/\mu)^2, \quad (2.4a)$$

$$\begin{aligned} t_N = & t(s = m^2, a) \\ = & \mu^2 (4m^2 - \mu^2) / (m^2 - a). \end{aligned} \quad (2.4b)$$

We note that as a ranges from zero to large negative values, the position of the nucleon pole in the t plane leaves the vicinity of the t -channel cut and approaches the s -channel cut as is shown in Fig. 2. Since we are to perform an extrapolation to the pole, it is reasonable to expect that it will become more reliable as the pole position is further removed from the t -channel cut. The motion of the pole toward the s -channel cut also contributes to the reliability of the extrapolation by decreasing the distance over which it must be made. In practice, however, a point is reached at which the value of a represents far forward center-of-mass angles for the low-energy region of integration and increasing $-a$ further becomes unprofitable. The range of a values involved in the present calculation as well as the relative extrapolation distances are shown in Fig. 2.

We now write Eq. (2.1) in the form in which we shall apply it:

$$\begin{aligned} 4\pi (2m/\mu)^2 X(t, a) = & \frac{t - t_N}{m^2 - a} [\text{Re}\tilde{B}^{(+)}(t, a) - I(t, a)] \\ = & G^2 + \frac{t - t_N}{m^2 - a} D(t, a). \end{aligned} \quad (2.5)$$

For $t \leq 0$ and $a \leq 0$, the real part and I can be calculated from πN phase shifts. The assumed smoothness of D as discussed above allows us to fit the calculated values of $X(t, a)$ for fixed a to a Taylor-series expansion in t about the point t_N ,

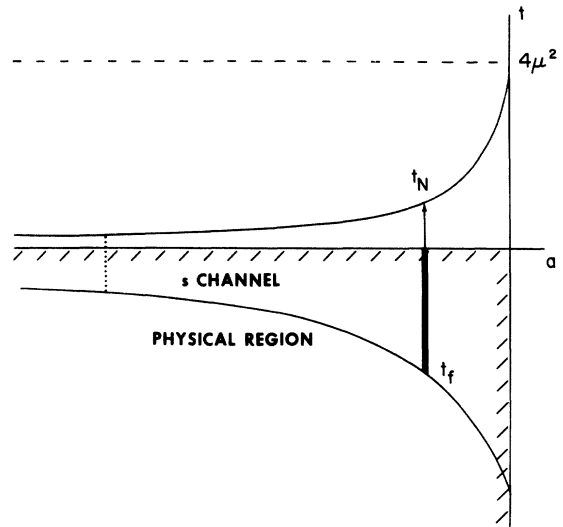


FIG. 2. The t - a plane showing the positions of the t -channel unitary cut and the nucleon pole as a function of a . Also shown are the curve $t_f(a, s)$ for $s = 2.56$ GeV², a typical range of t values (heavy vertical line) for which X values were calculated, and the extrapolation range (arrow). Note: The t scale below the a axis is 10× the scale above the axis. The vertical dotted line denotes the extent in a to which the calculation was done.

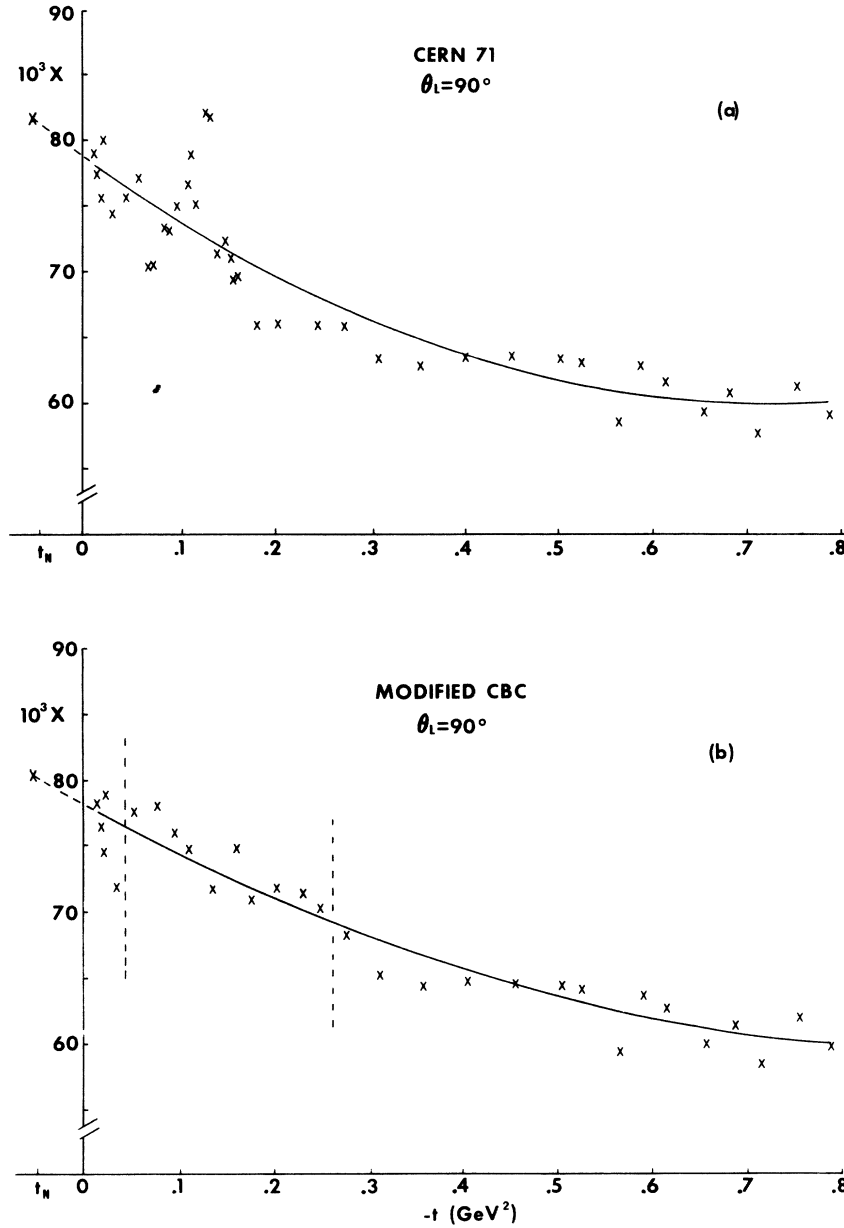


FIG. 3. The values obtained for $X(t, a)$ at $a = -0.86 \text{ GeV}^2$ ($\theta_L = 90^\circ$), and the fit and extrapolation to the nucleon pole for (a) the CERN 71 and (b) the modified CBC phase-shift solutions. The vertical dashed lines in (b) delineate the region in which CBC phase shifts are used.

at which only f^2 remains in the right-hand side of Eq. (2.5).

Fixing the value of a corresponds to fixing the laboratory scattering angle in the s -channel physical region:

$$\cos \theta_L = -\frac{a + m^2 - \mu^2}{[a^2 - \Sigma a + (m^2 - \mu^2)^2]^{1/2}}, \quad a \leq 0$$

where $\Sigma = 2(m^2 + \mu^2)$. It also corresponds to per-

forming the integration of $I(t, a)$ over a range of center-of-mass-system angles given by

$$\frac{a + s_0}{a - s_0} > \cos \theta_{\text{c.m.}} > \frac{a + s_c}{a - s_c},$$

where s_c is the value of s at which the integral is truncated. By varying a , we may perform the calculation over the entire region for which scattering data are available.

III. RESULTS

The analysis was performed for two sets of phase shifts: those of Almeded and Lovelace⁸ (CERN 71) and a mixture consisting of the Carter, Bugg, and Carter⁹ (CBC) solution over the range of energies for which it is given ($1.328 \text{ GeV}^2 \leq s \leq 1.744 \text{ GeV}^2$) and the CERN 71 solution at energy values above and below this range. The two solutions join smoothly at the higher connecting point, and a modification was made to the S_{11} partial wave to ensure a smooth connection at the lower point.

In Figs. 3(a) and 3(b), $X(t, a)$ as calculated from the left-hand side of Eq. (2.5) is plotted for the CERN 71 and modified CBC solutions, respectively, for fixed $a = -0.86 \text{ GeV}^2$ ($\theta_L = 90^\circ$). In order to avoid systematic errors arising from interpolation techniques, the evaluation was done only at values of t corresponding to energies at which the phase-shift solutions are given. Since in each case, the partial-wave analysis was made at energies at which the scattering data were available, the scatter in the points in Figs. 3(a) and 3(b), which is due primarily to scatter in the real parts, accurately represents the relative smoothness of the particular analysis. Interpolations for the purpose of performing the integrals were made with a spline technique. Here, the energy dependence is smoothed out and the integrals were essentially identical for the two phase-shift sets.

The smooth curves in Figs. 3(a) and 3(b) represent the polynomial fits to the calculated values of X . Also shown are the extrapolations to the nucleon pole where $X(t_N, a) = f^2$. Several criteria were applied to the selection of the proper order of the polynomial for which to perform the fit, and it was found that a quadratic was sufficient over

the ranges of a and t used. In the absence of any reliable estimate of the actual errors, all points were weighted equally.

In Fig. 3(b), the vertical dashed lines delineate the region in which the CBC phase shifts were used to calculate the real part of the amplitude. (CBC phase shifts were also used in this region in the calculation of the integrals for this solution.) This region represents the range of energies over which the $\Delta(1238)$ resonance contribution to the P_{33} partial wave is significant. Although the CERN 71 solution weights this region by twice as many points as does the CBC solution, the relative lack of smoothness of the former in the vicinity of the Δ is apparent. We determined that the Δ was responsible for approximately 70% of our result in both instances. Therefore, this region, as well as lower energies where s waves predominate, deserves careful attention in future partial-wave analyses. At the moment, however, we see no reason to favor either of the phase-shift sets we have used over the other, and our results are reported for both with no implication that they should be averaged.

The values of a for which the calculation has been performed are given, along with other relevant quantities, in Table II. Also given in Table II are the results of the extrapolations at these values for both sets of phase shifts. The quoted errors are determined by the χ^2 fitting procedure under the ansatz of equal weighting of the X values. The consistency of the results over the range of a values is shown graphically in Figs. 4(a) and 4(b). Weighted averages were taken in each case, yielding the values

$$f^2 = (81.5 \pm 1.5) \times 10^{-3} \quad (\text{CERN 71})$$

$$f^2 = (79.5 \pm 1.0) \times 10^{-3} \quad (\text{modified CBC}).$$

TABLE II. Values of a and other parameters for which calculations were performed, and results of the extrapolations. t_f is the greatest negative value of t for which $X(t, a)$ was calculated in each fit. The values given correspond to a constant value of s equal to 2.56 GeV^2 . All other quantities are defined in the text.

a (GeV^2)	θ_L (deg)	$\theta_{\text{c.m.}}$ (deg)	t_N (GeV^2)	t_f (GeV^2)	$10^3 f^2$ (CERN 71)	$10^3 f^2$ (modified CBC)
-12.2	30	34.2-64.4	0.00521	-0.182	82.5 ± 1.3	78.8 ± 1.3
-5.09	45	51.1-88.6	0.0114	-0.352	81.3 ± 1.3	79.2 ± 0.9
-2.61	60	67.4-107.4	0.0195	-0.521	80.8 ± 1.4	79.6 ± 0.9
-1.47	75	83.3-122.2	0.0290	-0.669	80.8 ± 1.4	79.8 ± 1.0
-0.860	90	98.6-134.3	0.0392	-0.788	80.9 ± 1.5	79.6 ± 1.0
-0.504	105	113.2-144.2	0.0493	-0.880	81.2 ± 1.5	79.5 ± 0.9
-0.284	120	127.4-152.8	0.0586	-0.948	81.6 ± 1.5	79.4 ± 1.0
-0.145	135	141.1-160.4	0.0665	-0.996	81.9 ± 1.6	79.3 ± 1.1
-0.061	150	159.2-167.2	0.0725	-1.028	82.2 ± 1.7	79.4 ± 1.3

IV. DISCUSSION

In this section we examine the advantages of the IDR method for calculating f^2 and recommend ways in which the uncertainty in this quantity can be further reduced.

a. Most prior determinations of f^2 from pion-nucleon data have involved the use of fixed- t dispersion relations or of some variation of them. The validity of these techniques is limited to the region of t in or very near to the forward scattering direction. In any other than a $t=0$ (forward) dispersion-relation calculation, where the integrals lie entirely within the physical region and total cross sections can be used to calculate them, it is necessary to extrapolate partial-wave expansions into the unphysical region. This extrapolation is in principle valid within the confines of the Lehmann ellipse, but in practice, where a finite number of terms are involved, uncertainties are introduced by the extrapolations of a truncated sum. While it is necessary to perform at least one extrapolation in any attempt to obtain f^2 , since the pole is at an unphysical point, it is desirable to limit the number of extrapolations to one. Since the IDR integral lies entirely within the physical region for any $a \leq 0$, only one extrapolation, that of $X(t, a)$ to $t=t_N$, is required.

b. For a given value of a , $\cos\theta_{c.m.}$ approaches -1 as s becomes large. This occurs rapidly for the values of a in our calculation, and one can therefore appeal to backward-scattering Regge pole models¹⁰ for information regarding the convergence of s -channel integrals. The πN invariant amplitudes have the behavior $t^{\alpha-1/2}$ for large $-t$, where $\alpha = \alpha_N$ or α_Δ depending upon the isospin of the amplitude. Since $\alpha_N \approx -0.03$ and $\alpha_\Delta \approx -0.37$, the integrals for all amplitudes are expected to converge. Particularly rapid convergence is expected for $\tilde{B}^{(+)} = B^{(+)}/\nu$, which has the asymptotic behavior $t^{\alpha-3/2}$, with the additional power of t provided by the factor of ν . This convergence has been verified numerically by us as we have determined, by incorporating a Regge parameterization,¹¹ that truncating the integral at the end of the partial-wave-solution energy range introduces an uncertainty in the value of the integral of less than 0.5%.

Indeed, because of both the rapid convergence of the integral and the fact that the integral residual is a smoothly and slowly varying function of t for $|t| \ll |t_c|$, where t_c is the value of t at the point of truncation, terminating the integral at even lower values of the integration variable results in negligible variations in our results. Thus, for example, truncating the integral at a point below where d , f , and higher partial waves become significant introduces a variation of less than 1% in

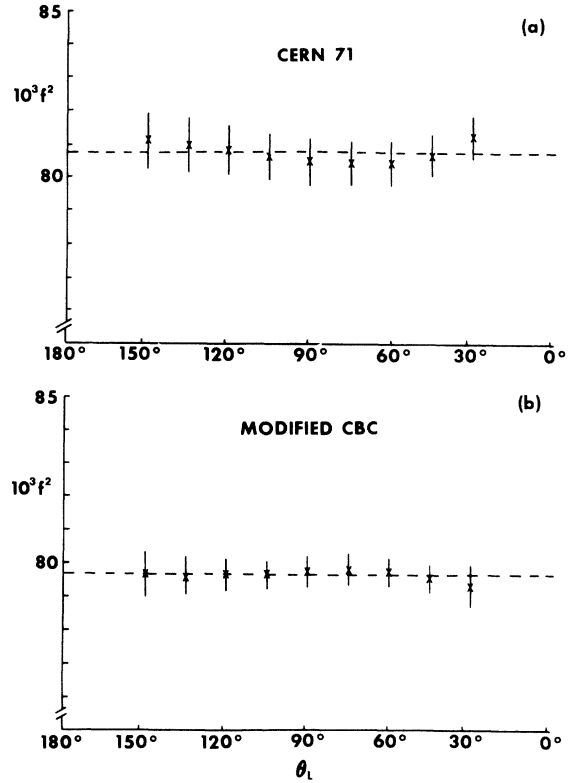


FIG. 4. Results of the extrapolations (see Table II).

the value of f^2 , even though the actual values of the integrals vary by a considerably larger fraction. This is because the residual

$$\Delta I(t, a) \equiv \frac{1}{\pi} \int_{-\infty}^{t_c} \text{Im} \tilde{B}^{(+)}(t', a) \frac{dt'}{t' - t},$$

being a smooth function of t , is effectively absorbed into the right-hand side of Eq. (2.5) with an appropriate redefinition of X :

$$\begin{aligned} 4\pi(2m/\mu)^2 X'(t, a) &\equiv \frac{t - t_N}{m^2 - a} [\text{Re} \tilde{B}^{(+)}(t, a) - I_c(t, a)] \\ &= G^2 + \frac{t - t_N}{m^2 - a} [D(t, a) + \Delta I(t, a)], \end{aligned}$$

where

$$I_c = I - \Delta I.$$

In our calculations, we integrated through the entire range of energies involved in the CERN 71 phase-shift solution, with the cutoff value of s being $s_c = 4.84 \text{ GeV}^2$. As we have seen above, X and X' differ by less than 0.5%, and we therefore estimate the resulting uncertainty in the value of f^2 to be less than 0.1%.

c. The variable a allows us an extra degree of freedom in which both to check the consistency of

our calculations and to sample the phase-shift solutions over the entire range of angles for which they were determined. This works to eliminate systematic errors due to overemphasis of the phase shifts in regions where they were not adequately constrained by data, particularly in the far forward and backward directions. Of special advantage here is the minimization of effects due to significant Coulombic corrections at forward angles.

Any calculation which requires an extrapolation has its pitfalls, and the present one is no exception. Except for certain model implications (locations of t -channel singularities, analyticity assumptions, etc.) the functional dependence of $X(t, a)$ for $t > 0$ is not known. Our smoothness assumption is at least as valid as any used in other techniques, but an improvement could be made by evaluating the t -channel integral using $\pi\pi$ phase shifts and/or meson singularity models. The extrapolation to the nucleon pole then becomes an interpolation. Efforts in this direction are being undertaken by the authors, but we believe that the extrapolations performed herein are valid within the accuracy of the phase-shift solutions at hand.

We also believe that the current level of accuracy obviates the necessity of explicitly taking into account the subthreshold $\pi N \rightarrow \gamma N$ contribution^{1, 5} to the s -channel unitary cut, particularly for the range of a and t values involved. This contribution is, in principle, included in our method since the discrepancy function D can be assumed to include the cut from $t=0$ to $t=t_N$ due to this process as well as the normal t -channel cut beginning at $t=4\mu^2$. A proper treatment would involve expanding D , or equivalently X , in an appropriate manner, i.e., in a series of functions having the cut structure. The principal effect here would be the introduction of a small imaginary part to X in the region between $t=0$ and $t=t_N$ along with a small cusp in the real part of X at these points. This cusp would be much smaller than the strong cusp¹² which appears in the real part of the invariant amplitude at threshold, and would not significantly affect the extrapolation of $\text{Re}X$ to the nucleon pole. On the other hand, if improved data make possible a reduction of the error in f^2 by a factor of 10 or more, the effects of the electromagnetic cuts, as well as those of isomultiplet mass differences, should be examined carefully.

An attempt was also made to extract f^2 in a similar manner from the amplitude $B^{(-)}$. An IDR can be written for $B^{(-)}(t, a)$ similar to that for $\bar{B}^{(+)}$; the Born term is now

$$B_{\text{IDR}}^{M^{(-)}}(t, a) = G^2 \frac{t_N - 2\mu^2}{(m^2 - a)(t - t_N)}.$$

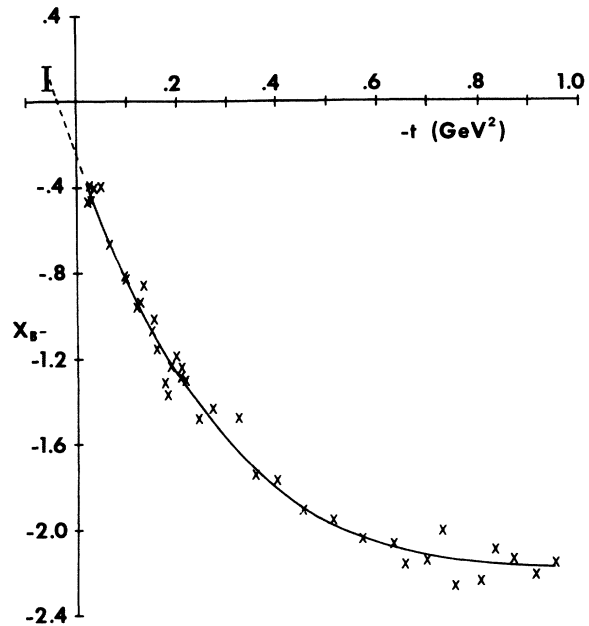


FIG. 5. Values of $X(t, a)$ at $a = -0.284 \text{ GeV}^2$ ($\theta_L = 120^\circ$) for $B^{(-)}$, the fit, and the extrapolation to the nucleon pole.

As can be seen in Fig. 5, however, the variation of $X_{B^-}(t, a)$ near the pole is too great for an accurate determination of f^2 to be made. A typical result is at $\theta_L = 120^\circ$ ($a = -0.284 \text{ GeV}^2$), where a value of $f^2 = (157 \pm 78) \times 10^{-3}$ was obtained. Although this value is within a standard deviation of the results obtained from $B^{(+)}$, it is clear that the choice of $B^{(-)}$ is not propitious for determining the coupling constant.

ACKNOWLEDGMENTS

We wish to thank Dr. William B. Kaufmann for several helpful discussions. One of us (G.E.H.) also wishes to thank the faculty and staff of the Department of Physics at Arizona State University for their hospitality.

APPENDIX

We present here some kinematical relationships pertinent to interior dispersion relations. For a more detailed account, the reader is referred to Ref. 7.

We use the conventional notation for the Mandelstam variables s , t , and u , m and μ for the nucleon and pion masses, and the definition $\nu \equiv s - u$. IDR's are written for amplitudes which are even functions of ν by fixing the value of the path parameter a , defined as

$$a = -\phi(s, t)/t^2,$$

where ϕ is the Kibble boundary function, and dispersing in t . As functions of t and a , s , u , and ν are given by

$$s(t, a) = \frac{1}{2}[\Sigma - t + \nu(t, a)],$$

$$u(t, a) = \frac{1}{2}[\Sigma - t - \nu(t, a)],$$

$$\nu(t, a) = [(t - 4\mu^2)(t - 4m^2) + 4at]^{1/2},$$

where $\Sigma = 2m^2 + 2\mu^2$. The change of integration variable is effected by the relationship

$$t(s, a) = -4sP_s^2/(s - a),$$

where

$$P_s^2 = [s - (m + \mu)^2][s - (m - \mu)^2]/4s$$

is the square of the s -channel center-of-mass momentum. Of particular value is the expression, for fixed a ,

$$(t' - t)(s' - a) = -(s' - s)(s' - u).$$

The s -channel center-of-mass scattering angle is given by

$$\cos\theta_{c.m.} = (a + s)/(a - s).$$

*Current address: Los Alamos Scientific Laboratory, Los Alamos, New Mexico 85744.

¹W. S. Woolcock, Nucl. Phys. **B75**, 455 (1974).

²D. V. Bugg, A. A. Carter, and J. R. Carter, Phys. Lett. **44B**, 278 (1973).

³R. Ayed and P. Bareyre, discussed by I. Butterworth, in proceedings of the Second International Conference on Elementary Particles, Aix-en-Provence, 1973 [J. Phys. (Paris) Suppl. **34**, C1-176 (1973)].

⁴N. Sznajder Hald, Nucl. Phys. **B48**, 549 (1972).

⁵V. K. Samaranayake and W. S. Woolcock, Nucl. Phys. **B48**, 205 (1972).

⁶G. Ebel *et al.*, Nucl. Phys. **B33**, 317 (1971).

⁷G. E. Hite, R. J. Jacob, and F. Steiner, Phys. Rev.

D **6**, 3333 (1972).

⁸S. Almeded and C. Lovelace, Nucl. Phys. **B40**, 157 (1972); CERN Report No. CERN TH 1408, 1971 (unpublished).

⁹J. R. Carter, D. V. Bugg, and A. A. Carter, Nucl. Phys. **B58**, 378 (1973).

¹⁰Vernon D. Barger and David B. Cline, *Phenomenological Theories of High Energy Scattering* (Benjamin, New York, 1969), Sec. 7.4, pp. 129-133.

¹¹E. L. Berger and G. C. Fox, Nucl. Phys. **B26**, 1 (1971); V. Barger and D. Cline, Phys. Rev. Lett. **21**, 392 (1968); **21**, 1132(E) (1968).

¹²G. Höhler, H. P. Jakob, and R. Strauss, Nucl. Phys. **B39**, 237 (1972).